Nuclear Engineering and Technology 54 (2022) 1588–1596

Contents lists available at ScienceDirect

Nuclear Engineering and Technology

journal homepage: www.elsevier.com/locate/net

Original Article

Prediction of fatigue crack initiation life in SA312 Type 304LN austenitic stainless steel straight pipes with notch

A. Ramachandra Murthy [a, *], S. Vishnuvardhan [a], K.V. Anjusha [b], P. Gandhi [a], P.K. Singh [c]

[a] CSIR-Structural Engineering Research Centre, Taramani, Chennai, India
[b] Vimal Jyothi Engineering College, Chemperi, Kerala, India
[c] Bhabha Atomic Research Centre, Trombay, Mumbai, India

ARTICLE INFO

Article history:
Received 14 September 2021
Received in revised form
21 October 2021
Accepted 12 November 2021
Available online 6 December 2021

Keywords:
Fatigue
Crack initiation life
Crack initiation models
Piping components
SA312 Type 304LN stainless Steel

ABSTRACT

In the nuclear power plants, stainless steel is widely used for fabrication of various components such as piping and pipe fittings. These piping components are subjected to cyclic loading due to start up and shut down of the nuclear power plants. The application of cyclic loading may lead to initiation of crack at stress raiser locations such as nozzle to piping connection, crown of piping bends etc. of the piping system. Crack initiation can also take place from the flaws which have gone unnoticed during manufacturing. Therefore, prediction of crack initiation life would help in decision making with respect to plant operational life. The primary objective of the present study is to compile various analytical models to predict the crack initiation life of the pipes with notch. Here notch simulates the stress raisers in the piping system. As a part of the study, Coffin-Manson equations have been benchmarked to predict the crack initiation life of pipe with notch. Analytical models proposed by Zheng et al. [1], Singh et al. [2], Yang Dong et al. [25], Masayuki et al. [33] and Liu et al. [3] were compiled to predict the crack initiation life of SA312 Type 304LN stainless steel pipe with notch under fatigue loading. Tensile and low cycle fatigue properties were evaluated for the same lot of SA312 Type 304LN stainless steel as that of pipe test. The predicted crack initiation lives by different models were compared with the experimental results of three pipes under different frequencies and loading conditions. It was observed that the predicted crack initiation life is in very good agreement with experimental results with maximum difference of ±10.0%.

1. Introduction

Fatigue is degradation mechanism that involves processes of crack initiation, its growth and fracture of components under repetitive stresses. This mechanism depends on the microstructural features of the material, loading amplitude and distribution of localized plastic deformation. The fatigue life of components/structures has broadly two phases, namely, crack initiation and crack growth periods as shown in Fig. 1. Crack initiation is mostly associated with cyclic plastic deformation which in turn is a function of stress raisers, sub-surface inclusion, gradient stress/strain field and environmental attack. Subsurface crack initiation has been observed primarily in many materials at very low stresses and very long lives, leading to the failure surface with the appearance of a fish-eye. Transition from surface-dominated fatigue processes to subsurface failure initiation is observed in the metals with primary inclusions. The difference in fatigue lives is significant between surface and sub-surface initiated modes of failure. Hence, the separation of experimental/analytical fatigue life data between surface and internal initiation failure modes is very important for several purposes, namely, tailored microstructural improvement at sensitive locations, repair, retrofitting and structural integrity assessment. The engineering fatigue crack initiation phase consists of three stages: crack nucleation, microstructurally and mechanically/physically short crack propagation [4,34]. Fig. 1 explains crack initiation period and the crack growth period until failure [5].

It is well known fact that the pipelines contain some defects during the manufacturing, installation and in-service. The significance of defects in the pipelines under various loading conditions is to be addressed properly for the design and safety assessment purposes. The pipelines are generally subjected to flexural fatigue loading due to which crack formation and growth will occur at defect/sensitive locations. The fatigue life of a pipe has two phases, namely, crack initiation and growth. Generally, crack spends about

* Corresponding author.
E-mail address: murthyarc@serc.res.in (A. Ramachandra Murthy).

https://doi.org/10.1016/j.net.2021.11.011

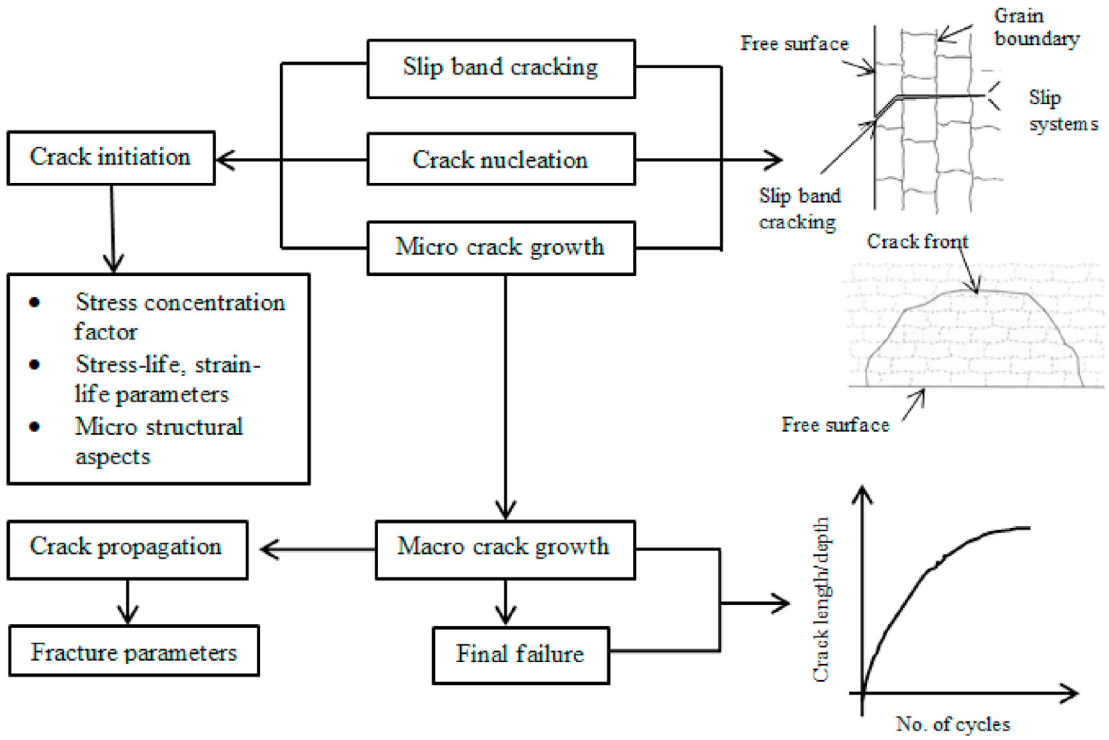

Fig. 1. Various phases of fatigue life and the associated factors.

40–60% of its life during crack initiation. From the wide literature, it was found that the analytical models to predict the crack initiation life of piping components are scanty.

The aspects related to fatigue crack initiation and short crack growth are not well understood. However long crack growth is well understood and is given by Paris Law. Many models were developed for crack growth analysis, remaining life prediction and residual strength evaluation of structural components [6]. With regard to quantitative analysis of crack initiation life, the variables that affect the crack initiation in components are many but limited evidences are reported covering merits and demerits of the existing models and the required input data. The crack initiation life is generally predicted based on the stress-life or strain-life curve obtained from failure of the smooth specimen tests under uni-axial cyclic loading. A transition crack size is assumed to be the divider between the crack initiation and propagation [7].

There are three major existing approaches, namely, stress-life, strain-life and microstructural based approach for prediction of crack initiation life. Brief details are presented in Table 1.

Both the models (stress-life and strain-life) do not contain parameters related to micro-structure in the fatigue-crack-initiation or the fatigue life. It has been observed that more investigations were reported on strain-life approach using the Coffin-Manson equation. The Coffin-Manson equation, which is on strain-based approach, is one of the most frequently-used models to predict low cycle fatigue (LCF) life of structural components. This has been applied to variety of problems such as structural materials, welding joint, new materials, multi-axial fatigue, thermal stress fatigue etc. [13–17].

Zheng et al. [18] predicted crack initiation life of LYI2CZ aluminum and 16 Mn steel using energy approach by relating the elastic-plastic stress and strain near a notch with the remotely applied stress. Various input parameters such as the elastic modulus, strength coefficient and strain hardening exponent were used in the formulation. Singh et al. [2] conducted studies on carbon steel pipes to validate the analytical procedures for evaluation of crack initiation life. Xie et al. [19] employed S-theory to determine crack initiation angle and critical load of circumferential periodic cracks in pipe. Meggiolaro et al. [20] performed statistical evaluation to arrive at Coffin-Manson parameters by using the monotonic tensile and uniaxial fatigue properties of 845 different metals, including 724 steels, 81 aluminium alloys, and 15 titanium alloys. Singh et al. [21] carried out fatigue studies on carbon steel piping materials and components of Indian Pressurized Heavy Water Reactors (PHWRs). The piping components include pipes and elbows, of outer diameter 219 mm, 324 mm and 406 mm, made of carbon steel (SA333 Gr.6 grade) material. The analytical predictions for both crack initiation and crack growth for the tested components were compared with the corresponding experimental results. Yan Dong et al. [25] proposed a relation between short crack initiation, propagation rate, mechanical properties, crack length, stress and strain. Benachour et al. [22] conducted fatigue crack initiation and propagation in notched plate made up of 2024 T351 Al-alloy under constant amplitude loading under tensile residual stress field. Mukhopadhyay et al. [23] described the use of acoustic emission (AE) and ultrasonic techniques for monitoring crack initiation/growth during ratcheting studies on a straight pipe made of 304LN austenitic stainless steel under reversed four-point bending. Huffman [24] proposed a strain energy based fatigue damage model to calculate stress-life, strain-life, and fatigue crack growth rates. Stress ratio effects intrinsic to the model are discussed, and parameterized in terms of the Walker equivalent stress and a fatigue crack growth driving force. Liu et al. [3] introduced a new method to predict the total fatigue life of notched components based on the theory of damage mechanics. The damage evolution equation of notched specimen under tension compression loading was obtained through closed-form solution. Ramachandra Murthy et al. [6] proposed a fatigue crack growth model for dissimilar metal weld joints of a piping component under cyclic loading, where in the crack is located at the center of the weld in the circumferential

Table 1
Approaches for prediction of fatigue crack initiation life.

Model	Details	Remarks
Stress-life ($S-N_f$) approach [8]	$\sigma_\alpha = \sigma'_f N_f^g$ Where, σ_α = the stress amplitude, σ'_f = fatigue-strength coefficient, N_f^g = the number of cycles to failure and α = the fatigue-strength exponent.	Failure is usually defined as (i) Compete fracture of the specimens or (ii) initiation of a fatigue crack to a certain length or depth.
Strain-life approach [9,10]	$\frac{\Delta\varepsilon_p}{2} = \varepsilon'_f N_f^b$ Where, ε'_f = the fatigue-ductility coefficient, and b = the fatigue-ductility exponent.	The plastic strain range ($\Delta\varepsilon_p$) related to the cycles to failure according to the Coffin-Manson relation. Failure is defined as complete fracture of specimen or life at the 75% drop in the load from maximum value.
Microstructural based approach Cheng and Laird [11]	$\frac{\Delta\gamma_p}{2} N_f^\alpha = C'$ Where, ($\Delta\gamma_p$) = plastic-shear-strain range, N_f = Crack initiation cycles and C' = a constant.	$\alpha = 0.78$, obtained by relating the slip offsets in the PSBs to the applied-strain amplitude. ranges from 0.5 to 1 (Venkataraman et al., 1991).
Microstructural based approach [12]	$(\Delta\tau - 2k)N_i^{1/2} = \left[\frac{8\mu W_s}{\pi d}\right]^{1/2}$ Where, $\Delta\tau$ is the shear-stress range, k is the friction stress of dislocation, μ is the shear modulus and d is the grain size	Wsis the specific fracture energy per unit area along the slip band.

direction. The fracture parameter, Stress Intensity Factor (SIF) has been computed by using principle of superposition.

In the present study, five existing analytical models for evaluation of crack initiation life have been discussed. The crack initiation life of three pipes with notch have been predicted using each of the five existing models. Brief descriptions about Coffin-Mansion equations and analytical procedure have been provided. As a part of the study, tension tests and strain-controlled fatigue tests have been conducted to evaluate tensile and fatigue properties parameters for SA312 Type 304LN stainless steel for use in evaluation of crack initiation life. Brief details of experimental studies carried out on SA312 Types 304LN stainless steel notched pipe under constant amplitude cyclic loading for determination of crack initiation life has also been discussed. The predicted and experimental crack initiation life has been compared.

2. Fatigue crack initiation models

The strain life approach relates deformation occurring in the immediate vicinity of a stress concentration to the remote or local pseudo-elastic stresses and strains with number of cycles to failure. It is known that fatigue crack initiation life strongly depends on metallurgical, geometrical, loading parameters, residual stress and the stress state in the vicinity of the defect. A relationship between total strain amplitude and number of cycles is given by Coffin-Manson equation. The constants of equation such as fatigue strength coefficient, fatigue strength exponent and fatigue ductility exponent are obtained by fitting the experimental data of elastic and plastic strain amplitude and number of cycles to failure.

The first step in predicting crack initiation life is to obtain a strain-life curve from smooth specimen fatigue tests, which defines the number of cycles required for failure of the specimens at given strain amplitude. Details of the strain life curves and their associated constants are explained below:

Total strain range can be decomposed into elastic and plastic and components.

Elastic component is obtained using Basquin equation (1910).

$$\frac{\Delta\varepsilon_{el}}{2} = \frac{\sigma'_f}{E}\left(2N_f\right)^b \tag{1}$$

Plastic component can be obtained using Coffin-Manson [9].

$$\frac{\Delta\varepsilon_{pl}}{2} = \varepsilon'_f\left(2N_f\right)^c \tag{2}$$

Relation between fatigue life and strain is shown in Fig. 2.

The total strain amplitude can be obtained as:

$$\frac{\Delta\varepsilon}{2} = \frac{\Delta\varepsilon_{el}}{2} + \frac{\Delta\varepsilon_{pl}}{2} \tag{3}$$

$$\frac{\Delta\varepsilon}{2} = \frac{\sigma'_f}{E}\left(2N_f\right)^b + \varepsilon'_f\left(2N_f\right)^c \tag{4}$$

The above equation is known as Coffin-Manson equation and to solve this equation for *Nf* for a given strain amplitude, number of iterations are required using numerical or graphical solutions.

$\frac{\Delta\varepsilon_{el}}{2}$ = Elastic strain amplitude,

$\frac{\Delta\varepsilon_{pl}}{2}$ = Plastic strain amplitude,

$\frac{\Delta\varepsilon}{2}$ = Total strain amplitude,

σ'_f = Fatigue strength coefficient,

$2N_f$ = Number of reversals to failure,

b = Fatigue strength exponent,

c = Fatigue ductility exponent.

σ'_f, b and c are to be obtained from experimental results

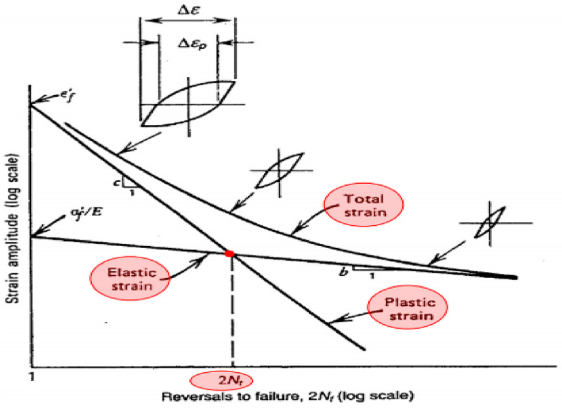

Fig. 2. Manson-Coffin-Basquin curve.

obtained from testing of polished, smooth specimens under fully reversible constant strain amplitude cycling and number of cycles to failure.

The second step in evaluating the crack initiation life is to determine the local stress and strain at stress raisers locations like at the notch root in notched plates. In case of notched plate, the fatigue notch factor, K_f can be used to evaluate the accurate strains at the notch root. Cyclic stress-strain equation for un-notched specimen is represented by a Ramberg-Osgood as given in Eq. (6).

$$\frac{\Delta\varepsilon}{2} = \frac{\Delta\varepsilon_{el}}{2} + \frac{\Delta\varepsilon_{pl}}{2} \tag{5}$$

$$\frac{\Delta\varepsilon}{2} = \frac{\Delta\sigma}{2E} + \left(\frac{\Delta\sigma}{2K'}\right)^{\frac{1}{n'}} \tag{6}$$

Where K' and n' are the cyclic strength coefficient and cyclic strain hardening exponent.

Third step is to evaluate the realistic local stress and strain using Neuber's rule.

According to Neuber's rule:

$$\Delta\varepsilon\,\Delta\sigma = K_f^2\,\Delta s\,\Delta e \tag{7}$$

For nominal elastic behavior:

$$\Delta e = \frac{\Delta s}{E} \tag{8}$$

$$\Delta\varepsilon\,\Delta\sigma = \frac{\left(K_f\,\Delta s\right)^2}{E} \tag{9}$$

Fourth step is to evaluate local strain considering cyclic stress strain of material from Eqs. (6) and (9).

Neuber's relation between nominal stress and notch stress is given in Eq .10.

$$\frac{(\Delta\sigma)^2}{E} + 2\,\Delta\sigma\left(\frac{\Delta\sigma}{2K'}\right)^{\frac{1}{n'}} = \frac{\left(K_f\,\Delta s\right)^2}{E} \tag{10}$$

Where $\Delta\varepsilon, \Delta\sigma$ are notch strain and stress ranges $\Delta s, \Delta e$ are nominal stress and strain range and Kf is fatigue notch factor. The above equation relates nominal stress range to notch stress range. Notch strain range, is then found from the hysteresis loop using Eq. (6).

Finally evaluate fatigue life using local strain (from Eq. (10)) and strain life curve (Eq. (4)). Alternatively, one can evaluate graphically.

In the present studies, five fatigue crack initiation models are compiled to predict the crack initiation life of pipes. These five models are proposed by Zheng et al. [1], Singh et al. [2], Yang Dong et al. [25], Masayuki et al. [33] and Liu et al. [3]. Brief description of the models is given below.

2.1. Model proposed by Zheng et al. [1]

Zheng et al. [1] proposed a local strain fracture model to predict fatigue crack initiation (FCI) life; the fatigue limit was taken into consideration. Similar to the macro-plastic yielding of metals, the model assumes a critical strain or stress level for cyclic loading, i.e., fatigue endurance limit strain. Further, the applied strain range $\Delta\varepsilon_p$ has been divided into two parts, i.e., the critical part $\Delta\varepsilon_C$ and the fatigue damage related part $\Delta\varepsilon_D$, i.e., $\Delta\varepsilon_p = \Delta\varepsilon_C + \Delta\varepsilon_D$. The modified Manson-Coffin formula proposed by Zheng et al. [1] is of the form:

$$\Delta\varepsilon_D = \Delta\varepsilon_p - \Delta\varepsilon_C = \beta N_f^{\gamma} \tag{11}$$

Further, an energy based modification to the local strain fracture model has also been proposed by Zheng et al. The proposed FCI accounted the several factors such as (i) the stress range $\Delta\sigma_o$, the endurance limit $\Delta\sigma_C$, the equivalent stress range $\Delta\sigma_{eqv}$, the equivalent endurance limit $(\Delta\sigma_{eqv})_{th}$, the fracture ductility ε_f, the elastic modulus E, the stress ratio R, the stress concentration factor K_t, the work-hardening coefficient K and the work-hardening exponent.

$$\text{Crack initiation life, } N_i = C\left[\left(\Delta\sigma_{eqv}\right)^{2/1+n} - \left(\Delta\sigma_{eqv}\right)_{th}^{2/1+n}\right]^{-2} \tag{12}$$

$$\text{Where } \Delta\sigma_{eqv} = \frac{K_t \times \Delta\sigma_o}{[2(1-R)]^{0.5}} \tag{13}$$

$$(\Delta\sigma_{eqv})_{th} \frac{K_t \times \Delta\sigma_c}{\left[2^{(1+n)} \times (1-R)^{(1-n)}\right]^{0.5}} \tag{14}$$

$$C = 0.25\varepsilon_f^2(\mathrm{EK})^{2/1+n}\left[\frac{2}{1+n}\right]^{2/1+n} \tag{15}$$

The FCI threshold, $\Delta\sigma_C$, is the upper limit of the stress amplitude, below or equal to which no fatigue damage occurs, and FCI life tends to infinity. Both C and $\Delta\sigma_C$ are material constants, and can be obtained from the tensile properties of metals.

2.2. Model proposed by Singh et al. [2]

The basis for the model proposed by Singh et al. [2] is Coffin-Manson's equation. It is assumed that the state of stress is plane 2D type. For the notch having tip radius, r and the remote stress range, $\Delta\sigma^0$, the approximate value of maximum pseudo elastic stress range $\Delta\sigma^{pe}$; at any distance, d (known as characteristic distance) from the notch tip can be determined by Creager's formula:

$$\Delta\sigma^{pe} = \frac{\Delta K}{\sqrt{2\pi r}}\left(1 + \frac{\rho}{2r}\right) \tag{16}$$

Where, $r = d + \frac{\rho}{2}$ ($\rho = 100\mu m$ based on cutter radius)

$$\Delta K = \Delta\sigma^0 \times \sqrt{\pi a} \times F_G \tag{17}$$

ΔK = Stress intensity factor range; a = Depth of the notch; F_G = Geometry factor, depends on the type of notch and shape of the component or specimen.

To predict the crack initiation life, the model considers the elastic–plastic strain range ahead of the crack tip, the distance (d) at which the representative strain range is to be determined also called the characteristic distance. The characteristic distance mentioned in the French A-16 guide is based on the hypothesis that for crack initiation from a blunt notch, finite volume of the material has to undergo damage. After evaluation of $\Delta\sigma^{pe}$, the corresponding pseudo elastic strain range is to be evaluated by using Eqn. (18), which approximately considers the state of tri-axial stress on the pseudo plastic strain range,

$$\Delta\varepsilon^{pe} = \frac{\Delta\sigma^{pe}}{E}\left[\frac{2(1+\mu)}{3}\right] \tag{18}$$

where μ is Poisson's ratio.

From the cyclic stress-strain and the pseudo elastic strain range, the total strain range is to be determined by using Neuber's rule (A16, 1995). Knowing the strain range, the number of cycles to crack initiation can be determined using the fatigue life curve given by Eq. (4).

2.3. Model proposed by Yang Dong et al. [25]

As per Yang Dong et al. [25]; fatigue crack initiation life can be predicted by:

$$N_{ip} = \left(\frac{\varepsilon_f}{\Delta\varepsilon}\right)^2 \ln\left(\frac{a_1}{a_1 - a^*}\right) \quad (19)$$

where, ε_f = True fracture strain, $\Delta\varepsilon$ = Total strain range; a_1 = Non-damaging crack length, a^* = Crack initiation length; N_{ip} = Predicted fatigue crack initiation life.

2.4. Model proposed by Masayuki et al. [33]

As per Masayuki et al. [33], fatigue crack initiation life can be predicted by:

$$lnN_{ip} = 3.794 - 2.202\ln(\varepsilon_a[\%] - 0.056) \quad (20)$$

where, ε_a = Strain amplitude.

2.5. Model proposed by Liu et al. [3]

Liu et al. [3] introduced a damage mechanics approach to estimate the crack initiation life. The damage evolution equation under tension-compression loading is obtained by closed-form solution. The fatigue crack initiation life is function of stress amplitude, stress concentration factor, notch depth, Young's modulus and notch tip radius. As per Liu et al. [3]; fatigue crack initiation life can be predicted as:

$$N_{ip} = p\left[\frac{\sigma(2k_t + 3)(r - a)^2}{5Er^2}\right]^{-\gamma} \quad (21)$$

where, the parameters p and γ are related to the loading conditions and material constantsand they can be obtained by fitting the existing experiment data; σ = Stress amplitude, K_t = Stress concentration factor; a = Notch depth, E = Young's modulus, r = Notch tip radius.

3. Experimental studies

3.1. Evaluation of tensile properties and fatigue parameters

Tensile properties of SA312 Type 304LN stainless steel used in the present studies were determined by carrying out tension tests as per ASTM E 8/E 8M [26]. Table 2 gives the tensile properties of SA312 Type 304LN stainless steel and the minimum required values as per ASTM A 312/A 312M [27]. The average yield strength and ultimate tensile strength of the material are found to be 315 MPa and 614 MPa respectively. The Young's Modulus and percentage elongation of the material are 198 GPa and 46 respectively [28]. Fig. 3 shows typical stress-strain plots obtained for SA312 Type 304LN stainless steel.

For carrying out low cycle fatigue tests, the specimens were fabricated from a pipe of 324 mm outer diameter and 25 mm wall thickness. ASTM E 606/E 606M [29] was followed in deciding the test specimens and carrying out fatigue tests. Specimen with uniform gauge test section of overall length of 220 mm was used; diameter at the gauge section was 8 mm and diameter at the grip section was 16 mm. Low cycle fatigue tests were carried out under strain control, using a ±250 kN capacity servo-hydraulic UTM. UTM has a self-restraining frame to which the load cell is mounted with necessary hydraulic grips for fixing the test specimen. The load cell measures and controls the applied load. UTM has an inbuilt Linear Variable Differential Transformer (LVDT) for measuring the actuator displacement. A dynamic rated extensometer having a range of +12.5 mm (extension) and −2.5 mm (compression) was used to measure longitudinal deformation in the uniform gauge test section and control strain amplitude. Hong et al. [30] indirectly measured strain in the gauge section using a linear variable differential transformer (LVDT) attached at the shoulders of the specimen. The strains in the gauge section were calculated from the values between the shoulders using the correlation between the two values which was established before the test.

Table 2
Mechanical properties of SA312 Type 304LN stainless steel.

Properties	Tested values	ASTM A 312/A 312M – 09 (min.)
Yield strength (MPa)	315	205
Ultimate strength (MPa)	614	515
Young's modulus (GPa)	195	–
% Elongation	46	25

Low cycle fatigue tests were carried out at room temperature and in air environment. The cyclic strain amplitude values during the tests were ±0.20%, ±0.35%, ±0.50%, ±0.65%, ±0.80% and ±0.95%. Table 3 presents the details of low cycle fatigue tests. The tests were carried out under constant strain amplitude loading with fully reversed cycling. A triangular wave pattern was employed during testing. The test frequency was maintained at 0.5 Hz. During the tests, the applied strain amplitude, corresponding load (or stress) and the number of cycles were continuously recorded using a computerised data logging system. The acquired data was used to obtain the stress-strain hysteresis curves. The tests were continued till the specimens failed. The numbers of cycles to failure were recorded for each test. The failure was defined as total separation or fracture of the specimen into two parts. Table 4 presents the number of cycles to failure (N_f) and number of reversals to failure ($2N_f$) for all the specimens.

A very low fatigue life of 397 cycles was observed for the specimen LCFTS16-8-4, which was tested at ±0.95% of strain amplitude and the highest fatigue life of 58505 cycles was observed for the specimen LCFTS16-8-6, which was tested at ±0.20% of strain amplitude. From the low cycle fatigue tests, strain-life curve and mid-life cyclic stress-strain hysteresis curves were obtained for SA 312 Type 304LN stainless steel. Fig. 4 shows superimposed mid-life

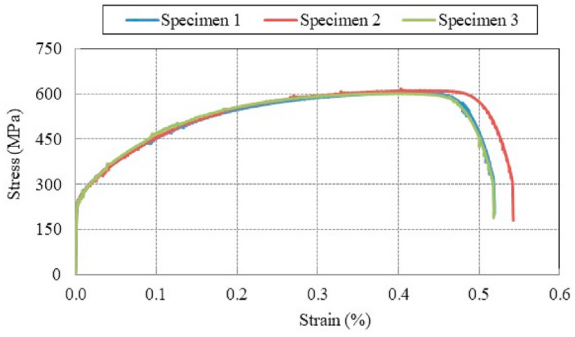

Fig. 3. Typical engineering stress-strain plots for SA312 Type 304LN stainless steel obtained from tension tests.

Table 3
Low cycle fatigue tests on SA312 Type 304LN stainless steel.

Specimen ID	Applied strain amplitude (%)	Maximum load range (kN)	Number of cycles to failure, N_f	Number of reversals to failure, $2N_f$
LCFTS16-8-1	±0.50	41.69	2583	5166
LCFTS16-8-2	±0.65	44.21	1267	2534
LCFTS16-8-3	±0.80	46.10	883	1766
LCFTS16-8-4	±0.95	49.82	397	794
LCFTS16-8-5	±0.35	36.17	5566	11132
LCFTS16-8-6	±0.20	30.90	58505	117010

Table 4
Fatigue and cyclic stress-strain constant parameters.

Fatigue parameter	Type 304LN (present studies)	Type 304L [31]
Cyclic strength coefficient, K' (MPa)	477	434/4742 (bilinear fit)
Cyclic strain hardening exponent, n'	0.3103	0.1106/0.5121 (bilinear fit)
Fatigue strength coefficient, σ_f' (MPa)	1134	330/1890 (bilinear fit)
Fatigue strength exponent, b	−0.1416	−0.0373/-0.2040 (bilinear fit)
Fatigue ductility coefficient, ϵ_f'	0.1605	0.1325
Fatigue ductility exponent, c	−0.4548	−0.3738

cyclic stress-strain hysteresis curves obtained at different strain amplitudes. Using the cyclic stress-strain components evaluated rom the test data and the numbers of reversals to failure, fatigue and cyclic stress-strain constant parameters were determined. Table 4 gives details of fatigue and cyclic stress-strain constant parameters obtained for SA 312 Type 304LN stainless steel.

3.2. Fatigue tests on SA312 Type 304LN straight pipes with notch

Fatigue tests were conducted on SA312 Type 304LN stainless steel straight pipes containing part-through notch [32]. Fig. 5 shows details of pipe specimen with notch. Fig. 6 shows a set-up for fatigue test on a straight pipe. All the tests were conducted under load control. Details of pipe specimens and fatigue tests are given in Table 5. Crack initiation lives obtained for the fatigue tests on pipes with notch are also given in Table 5.

Crack initiation in the pipe specimens was monitored using a crack measuring gauge which works based on ACPD technique. Crack initiation life is number of cycles corresponding to crack growth of approximately 0.1–0.5 mm. The difference in crack initiation life of pipe specimens is attributed to applied stress range and stress ratio.

4. Results and discussion

The predicted crack initiation life by all the five models is presented in Tables 6–10. Table 11 compares the predicted crack initiation life by five models with the corresponding experimental values. Experimental fatigue crack initiation life for pipe specimens 1, 2 and 3 are 4000, 3500 and 3250 cycles respectively. From Table 11, it can be observed that (i) the predicted crack initiation life by all the models is in very good agreement with the corresponding experimental observations except for the specimen 1 by the model proposed by Zheng et al. [1] and (ii) the maximum % difference with respect to experimental observation is ±10.12%.

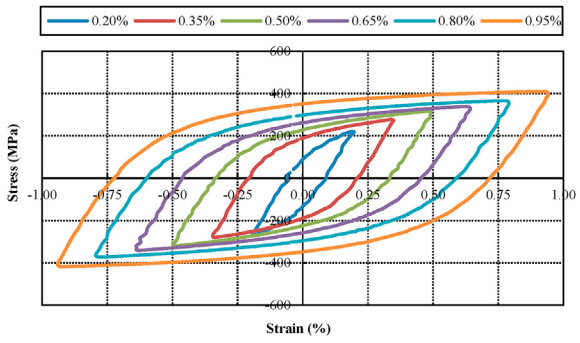

Fig. 4. Mid-life cyclic stress-strain hysteresis curves for SA312 Type 304LN stainless steel.

Equivalent stress range for specimen 2 is higher when compared with the other two specimens. In general, higher stress range would result in lesser number of cycles for crack initiation. While the number of cycles for crack initiation in specimen 1 is higher than specimen 2, the same is lower for specimen 3 for which the equivalent stress range is lower compared to specimen 2. This could be due to difference in stress ratio. While specimens 1 and 2 has mean stress, specimen 3 has no mean stress. However, the model proposed by Zheng et al. [1] has not considered the effect of mean stress in predicting crack initiation life.

The model proposed by Zheng et al. [1] predicted the fatigue crack initiation life for three notched pipes by considering the several aspects such as equivalent stress range, equivalence endurance limit, fatigue strength coefficient. The predicted crack initiation lives are 4925, 3625 and 3322 cycles respectively. Singh et al. [2] model predicted the crack initiation life based on fracture mechanics concept, pseudo plastic strain range and elastic strain range. The predicted crack initiation life is 4006, 3606 and 3280 cycles respectively. Yang Dong et al. [25] model predicted the crack initiation life by considering the true fracture strain and total strain. The predicted crack initiation life is 3692, 3439 and 3224 cycles respectively. The model proposed by Masayuki et al. [33] predicted the fatigue crack initiation life by considering the stress and strain amplitude. The predicted crack initiation life is 4405, 3714 and 3170 cycles respectively. The model proposed by Liu et al. [3] predicted the fatigue crack initiation life by considering the stress amplitude, notch configuration, stress concentration factor. The predicted crack initiation life is 4121, 3707 and 3320 cycles respectively.

Possible reasons for the difference between the predicted and the experimental life include (i) considering the same value of non-damaging crack length for all the pipes (ii) calculation of geometric factor by using a specific method (RCC-MR) (iii) approximating the notch tip radius and (iv) approximations in calculation of stress concentration factor. Based on the input data available for the specific material, the models can be used for prediction of crack initiation life. The predicted crack initiation life will be very much useful to

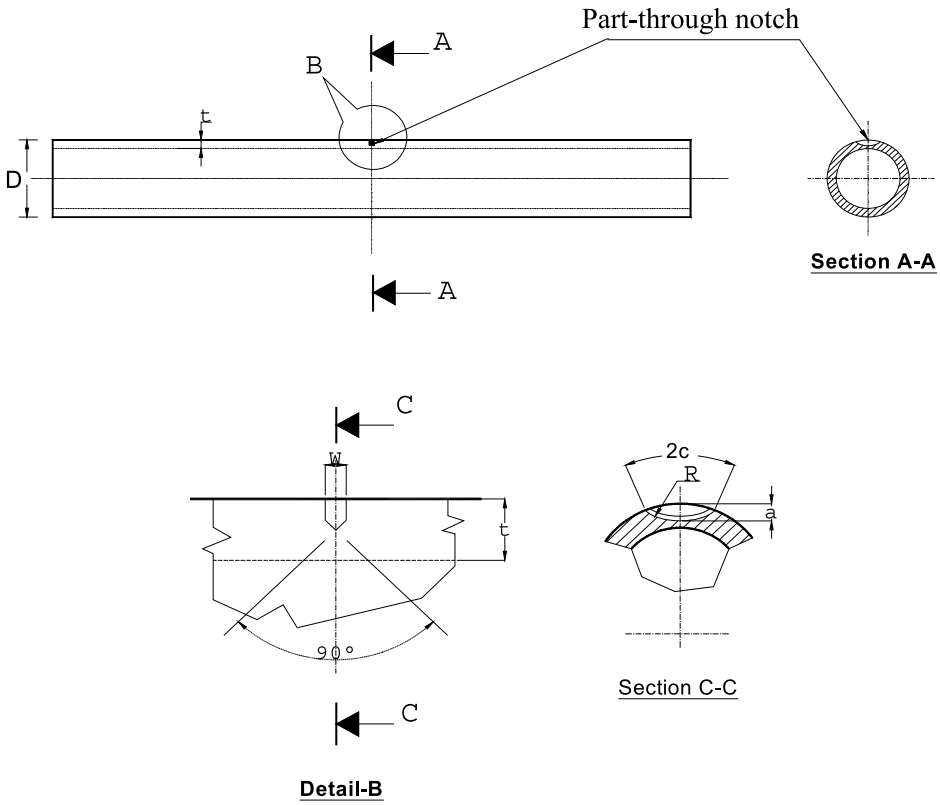

Fig. 5. Details of pipe specimen with notch.

Fig. 6. Set-up for fatigue test on a straight pipe.

make several decisions such as (i) tailored microstructure at sensitive locations (ii) repair and retrofitting (iii) structural integrity assessment and damage tolerant design of structures/components.

5. Conclusions

- In the present study, fatigue crack initiation life has been evaluated analytically and experimentally for the straight pipes with notch. Coffin-Manson equations have been outlined and benchmarked to predict the crack initiation life of straight pipes with notch.
- To predict the fatigue crack initiation life of piping components under constant amplitude flexural loading, the models proposed by Zheng et al. [1], Singh et al. [2], Yang Dong et al. [25], Masayuki et al. [33] and Liu et al. [3] have been compiled.
- Tensile and fatigue parameters were evaluated for SA312 Type 304LN stainless steel by conducting tension tests and strain-controlled fatigue tests.
- Experimental fatigue crack initiation life was determined for three piping components made up of SA312 Type 304LN stainless steel under different loading and frequency conditions.
- Fatigue crack initiation life is predicted for all the three pipes analytically by using five models. It was observed that the predicted crack initiation life is in very good agreement with the corresponding experimental life. The maximum % difference is observed as±10.12%.
- From the overall study, it can be summarized that the model proposed by Masayuki et al. [33] requires simple input, namely, Young's modulus, stress amplitude and strain amplitude for the prediction of crack initiation life.
- The model proposed by Singh et al. [2] is strongly based on fracture mechanics principles and the predicted life by using this method is reliable. All other models involve some empiricism and approximation.
- The predicted crack initiation life will be very much useful to make several decisions such as (i) tailored microstructure at

Table 5
Geometry, loading and crack initiation life of pipe specimens.

Details of pipe specimens		Specimen 1	Specimen 2	Specimen 3
Outer diameter of pipe, D (mm)		169	168	168
Inner span (mm)		680	680	680
Outer span (mm)		1700	1700	1700
Nominal Thickness of pipe, t (mm)		15.08	15.3	14.64
Length of the pipe, L (mm)		2005	2004	2005
Direction of notch		Circumferential	Circumferential	Circumferential
Type of notch		Part-through	Part-through	Part-through
Initial notch dimensions (mm)	Length, 2C (mm)	36	36	36
	Width, W (mm)	2	2	2
	Depth, a (mm)	3.55	3.61	3.62
	Tip radius, r_t (mm)	0.1	0.1	0.1
	Notch angle, 2 θ (°)	24.41	24.55	24.55
Frequency (Hz)		0.1–0.3	0.15–0.3	0.2
Cyclic load (kN)	Maximum	258	129	129
	Minimum	25.8	258	−129
Load ratio		0.1	0.5	−1
load range (MPa)		232.2	129.0	258.0
Stress range (MPa)		400.58	338.58	630.46
Crack initiation life (cycles)		4000	3500	3250

Table 6
Predicted life by using the model proposed by Zheng et al. [1].

Parameters	Specimen 1	Specimen 2	Specimen 3
Nominal applied stress range, $\Delta\sigma_o$ (MPa)	400.58	338.58	630.46
Stress ratio, R	0.1	0.5	−1
Equivalent stress range, $\Delta\sigma_{eqv}$ (MPa)	298.57	338.58	315.23
Equivalent endurance limit, $(\Delta\sigma_{eqv})_{th}$ (MPa)	115.24	141.13	87.5
Predicted fatigue crack initiation life, N_{ip} (No. of cycles)	4925	3625	3322

Table 7
Predicted life by using the model proposed by Singh et al. [2].

Parameters	Specimen 1	Specimen 2	Specimen 3
Remote stress range, $\Delta\sigma^{\circ}$ (MPa)	400.57	338.58	630.47
Geometry factor, F_G	0.679	0.873	0.390
Depth of the notch, a (mm)	3.55	3.61	3.62
Stress intensity factor range, ΔK	908.317	995.43	829.41
Maximum pseudo elastic stress range, $\Delta\sigma^{pe}$(MPa)	1481.92	1624.04	1353.18
Pseudo plastic strain range, $\Delta\epsilon^{pe}$	0.006586	0.007218	0.006014
Elastic strain range, $\Delta\epsilon_e$	0.002054	0.001736	0.003233
Total strain range, $\Delta\epsilon$	0.008641	0.008954	0.009247
Predicted fatigue crack initiation life, N_{ip} (No. of cycles)	4006	3606	3280

Table 8
Predicted life by using the model proposed by Yang Dong et al. [25].

Parameters	Specimen 1	Specimen 2	Specimen 3
True fracture strain, ε_f	0.508	0.508	0.508
Total strain range, $\Delta\varepsilon$	0.008641	0.008954	0.009247
Non-damaging crack length, a_1 (mm)	55	55	55
Crack initiation length, $a^{\times}$(mm)	36.1	36.1	36.1
Predicted fatigue crack initiation life, N_{ip} (No. of cycles)	3692	3439	3224

Table 9
Predicted life by using the model proposed by Masayuki et al. [33].

Parameters	Specimen 1	Specimen 2	Specimen 3
Young's modulus, E (GPa)	195	195	195
Stress amplitude, σ (MPa)	200.29	169.29	315.23
Strain amplitude, ε_a (%)	0.18	0.19	0.2
Predicted fatigue crack initiation life, N_{ip} (No. of cycles)	4405	3714	3170

Table 10
Predicted life by using the model proposed by Liu et al. [3].

Parameters	Specimen 1	Specimen 2	Specimen 3
Young's modulus, E (GPa)	195	195	195
Stress amplitude, σ (*MPa*)	200.29	169.29	315.23
Notch tip radius, r (mm)	0.1	0.1	0.1
Notch depth, a (mm)	3.55	3.61	3.62
Stress concentration factor, K_t	3.4	4.2	1.6
P	7.918×10^5	7.918×10^5	7.918×10^5
γ	6.0174	6.0174	6.0174
Predicted fatigue crack initiation life, N_{ip} (No. of cycles)	4121	3707	3320

Table 11
Comparison of analytical and experimental results.

Model/Experimental	No. of cycles for crack initiation & (Percentage error in prediction)		
	Specimen 1	Specimen 2	Specimen 3
Zheng et al. [1]	4925 (−23.1%)	3625 (−3.5%)	3322 (−2.21%)
Singh et al. [2]	4006 (−0.15%)	3606 (−3.02%)	3280 (−0.92%)
Yang Dong et al. [25]	3692 (7.7%)	3439 (1.74%)	3224 (0.8%)
Masayuki et al. [33]	4405 (−10.12%)	3714 (−6.11%)	3170 (2.46%)
Liu et al. [3]	4121 (−3.02%)	3707 (−5.91%)	3320 (−2.15%)
Experimental crack initiation life (Cycles)	4000	3500	3250

sensitive locations (ii) repair and retrofitting (iii) structural integrity assessment and damage tolerant design of structures/components.

Declaration of competing interest

The authors declare that they have no known competing financial interests or personal relationships that could have appeared to influence the work reported in this paper.

References

[1] M. Zheng, J.H. Luo, X.W. Zhao, Z.Q. Bai, R. Whang, Effect of pre-deformation on the fatigue crack initiation life of X60 pipeline steel, Int. J. Pres. Ves. Pip. 82 (2005) 546–552.
[2] P.K. Singh, K.K. Vaze, V. Bhasin, H.S. Kushwaha, P. Gandhi, D.S. Ramachandra Murthy, Crack initiation and growth behaviour of circumferentially cracked pipes under cyclic and monotonic loading, Int. J. Pres. Ves. Pip. 80 (2003) 629–640.
[3] Jianhui Liu, Yaobing Wei, Chagfeng Yan, Shanshan Lang, Method for predicting crack initiation life of notched specimen based on damage Mechanics, J. Shanghai Jiaot. Univ. 23 (2018) 286–290.
[4] S. Suresh, R. Ritchie, Propagation of short fatigue cracks, Int. Met. Rev. 29 (1) (1984) 445–475.
[5] Jaap Schijve, The significance of fatigue crack initiation for predictions of the fatigue limit of specimens and structures, Int. J. Fatig. 61 (2014) 39–45.
[6] A. Ramachandra Murthy, P. Gandhi, S. Vishnuvardhan, G. Sudharshan, Crack growth analysis and remaining life prediction of dissimilar metal pipe weld joint with circumferential crack under cyclic loading, Nuc. Eng. Techn. 52 (2020) 2949–2957.
[7] D. Radaj, C.M. Sonsino, W. Fricke, Fatigue Assessment of Welded Joints by Local Approaches, Woodhead Publishing, 2006.
[8] M.R. Mitchell, in: M. Meshii (Ed.), Fatigue and Microstructure, ASM, Metals Park, OH, 1978, pp. 385–437.
[9] L.F. Coffin Jr., Trans. ASME 76 (1954) 931–950.
[10] S.S. Manson, M.H. Hirschberg, Fatigue: an Inter-disciplinary Approach, Syracuse University, Syracuse, NY, 1964, pp. 133–178.
[11] A.S. Cheng, C. Laird, Fatig. Fract. Eng. Mater. Struct. 4 (1981) 343–353.
[12] K. Tanaka, T. Mura, ASME J. Appl. Mech. 48 (1981) 97–103.
[13] P. Darcis P, T. Lassen T, N. Recho, Fatigue behavior of welded joints - Part 2: Physical modeling of the fatigue process, Weld. J. 85 (2006) 19.S–26.S.
[14] M.A. Jameel, P. Peralta, C. Laird, Initiation and propagation of stage-I cracks in copper single crystals under load control, Mater. Sci. Eng. A342 (2003) 279–286.
[15] N. Gao, M.W. Brown, K.J. Miller, An effective method to investigate short crack growth behaviour by reverse bending testing, Int. J. Fatig. 29 (2007) 565–574.
[16] M. Weick, J. Aktaa, Microcrack propagation and fatigue lifetime under non-proportional multiaxial cyclic loading, Int. J. Fatig. 25 (2003) 1117–1124.
[17] F.A. Kandil, M.W. Brown, K.J. Miller, Biaxial Low-Cycle Fatigue Fracture of 316 Stainless Steel at Elevated Temperature, 280, Metals Soci, London, 1982, pp. 203–210.
[18] M. Zheng, E. Niemi, X. Zheng, An approach to predict fatigue crack initiation life of LY12CZ aluminium and 16 Mn steel, Theor. Appl. Fract. Mech. 26 (1997) 23–28.
[19] Y.J. Xie, X.H. Wang, Crack initiation and direction for circumferential periodic cracks in pipe under tension and torsion, Theor. Appl. Fract. Mech. 40 (2003) 153–159.
[20] M.A. Meggiolaro, J.T.P. Castro, Statistical evaluation of strain-life fatigue crack initiation predictions, Int. J. Fatig. 26 (2004) 463–476.
[21] P.K. Singh, V. Bhasin, K.K. Vaze, A.K. Ghosh, H.S. Kushwaha, D.S.R. Murthy, P. Gandhi, S. Sivaprasad, Fatigue studies on carbon steel piping materials and components: Indian PHWRs, Nucl. Eng. Des. 238 (2008) 801–813.
[22] M. Benachour, N. Benachour, M. Benguediab, Fatigue crack initiation and propagation through residual stress field, Int. Scholarly and Scientific Res. Innovation 6 (2012) 2470–2474.
[23] C.K. Mukhopadhyay, T. Jayakumar, T.K. Haneef, S. Suresh Kumar, B.P.C. Rao, Sumit Goyal, Suneel K. Gupta, Vivek Bhasin, S. Vishnuvardhan, G. Raghava, P. Gandhi, Use of acoustic emission and ultrasonic techniques for monitoring, Int. J. Pres. Ves. Pip. 116 (2014) 27–36.
[24] P.J. Huffman, A strain energy based damage model for fatigue crack initiation and growth, Int. J. Fatig. 88 (2016) 197–204.
[25] H.U. Yang Dong, H.U. Zhi Zhong, C.A.O. Shu Zhen, Theoretical Study on Manson-Coffin Equation for Physically Short Cracks and Lifetime Prediction, Science China Technological Sciences, 2011, pp. 1–9.
[26] ASTM E 8/E8M - 15, Standard Test Methods for Tension Testing of Metallic Materials [Metric], ASTM International, USA.
[27] ASTM A 312/A 312M - 09, Standard Specification for Seamless, Welded and Heavily Cold Worked Austenitic Stainless Steel Pipes, ASTM International, USA.
[28] Bhavana Joy, S. Vishnuvardhan, G. Raghava, P, P. Gandhi, Mathews M. Paul, Low cycle fatigue characteristics of SS 304 LN stainless steel, in: *Proceedings of the 2nd International Conference on Materials for the Future*, Thrissur, India, February 23-25, 2011.
[29] ASTM E 606/E 606M - 12, Standard Test Method for Strain-Controlled Fatigue Testing, ASTM International, USA.
[30] J.-D. Hong, C. Jang, T.S. Kim, Effects of mixed strain rates on low cycle fatigue behaviors of austenitic stainless steels in a simulated PWR environment, Int. J. Fatig. 82 (2016) 292–299.
[31] J. Colin, A. Fatemi, S. Taheri, Fatigue behaviour of stainless steel 304L including strain hardening, prestraining, and mean stress effects, J. Eng. Mater. Technol. 132 (2010) 1–13.
[32] G. Raghava, P. Gandhi, K.K. Vaze, Cyclic fracture, FCG and ratcheting studies on Type 304LN stainless steel straight pipes and elbows, Procedia Engineering 55 (2013) 693–698.
[33] Masayuki Kamaya, Fatigue crack tolerance design for stainless steel by crack growth analysis, Eng. Fract. Mech. 177 (2017) 14–32.
[34] U. Zerbst, M. Madia, M. Vormwald, H.T. Beier, Fatigue strength and fracture mechanics - a general perspective, Eng. Fract. Mech. 198 (2018) 2–23.